Experimental investigation of scatterer-array-based decorrelation technique applied to real multiple-input multiple-output base station

Yipeng Wang,[1] Xiaoyu Huang,[1] Jianyao Zhao,[2]
Zhimeng Zhong,[2] Wei E.I. Sha,[3] and Xiaoming Chen[1,✉]

[1] *School of Information and Communications Engineering, Xi'an Jiaotong University, Xi'an, China*
[2] *RAN Research Department, Huawei Technologies Co., Lts., Shanghai, China*
[3] *College of Information Science and Electronic Engineering, Zhejiang University, Hangzhou, China*

✉Email: xiaoming.chen@mail.xjtu.edu.cn

In this paper, a scatterer-array-based decorrelation method for improving the multiple-input multiple-output (MIMO) performance is proposed for a real application of base station (BS) operating at 780 MHz with a 20-MHz communication bandwidth. The antenna correlation is reduced by loading a scatterer array designed to increase the MIMO array's effective inter-element spacing. As a result, the diversity measure is improved, which in turn benefits the MIMO capacity. This method is demonstrated first in simulation to check its performance, which shows about 4% and 20% improvements in MIMO capacity over 20-MHz communication bandwidth in single-cell and multi-cell scenarios, respectively. Then it is applied to a real BS in a realistic urban micro scenario for experimental verification, showing a noticeable throughput improvement without degrading the power coverage of the BS. Note that this is the first time that the scatterer-array-based decorrelation technique has been applied to increase the MIMO throughput of a real BS in a real-life scenario, which thoroughly demonstrates the promising application potential of this technique.

Introduction: Multiple-input multiple-output (MIMO) antennas are at the core of modern telecommunications [1–6]. The industry has made extensive efforts to design MIMO systems and large MIMO antenna arrays. However, due to the high correlation of the array antenna in real multipath scenarios [2, 3], there is still room for improving its MIMO performance. Nevertheless, focusing only on improvements in traditional antenna characteristics, such as isolation enhancements, cannot ensure significantly improved MIMO performance [7, 8]. Some works attempted to lower the correlation from the perspective of antenna array design [9–11]. However, these studies assumed an isotropic scattering environment, which is not a realistic assumption for applications of the base station (BS). Besides antennas, space limitation and limited angular spread of the propagation channel are two main factors that affect the antenna correlation in a MIMO array [2, 5]. Therefore, from the joint of electromagnetic wave propagation and array antenna design, improving MIMO performance based on reducing the correlation of array antennas is valuable work.

For a BS with limited angular spread, a brilliant idea to enhance the MIMO capacity by reducing the antenna correlation is to make the radiation patterns orthogonal to each other under a given incoming wave distribution [12, 13]. However, the former work only provided a theoretical result, and it did not concern how to implement it in reality. The latter work assumed a free space environment and was only demonstrated using single-cell simulation. The BS array configuration was experimentally studied in [14]. It is well known that an antenna array with larger inter-element spacing tends to have lower antenna correlations in a fixed multipath environment. From the joint antenna-propagation perspective, the authors in [7, 15] proposed decorrelation techniques, which enhanced the MIMO performance in multipath environments by adding scatterers in front of the antenna array. This kind of decorrelation method utilizes the array's aperture without changing the existing structure of the antenna array. Nevertheless, it has only been validated for simple patch arrays using single-cell simulation. Its effectiveness on a real BS array in a more realistic multipath environment has not been demonstrated to date.

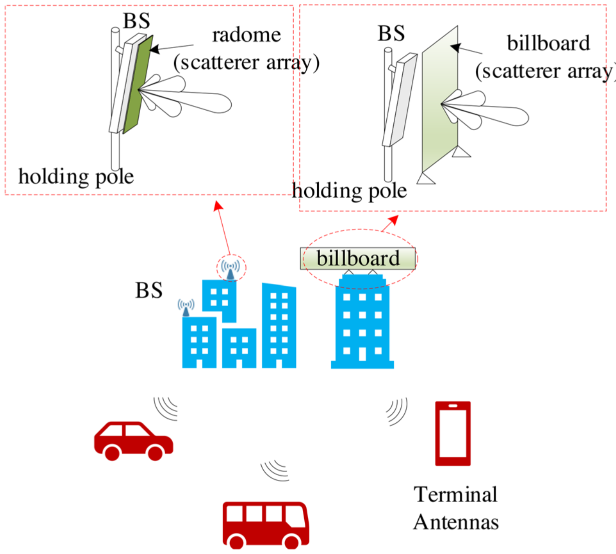

Fig. 1 *Applications of proposed scatterer array in UMi scenario as radome or billboard. UMi, urban micro.*

In this paper, a scatterer array is designed, fabricated, and applied to a real BS array using the method proposed in [15]. The main contributions of this letter are listed as follows:

1. Unlike the simple 1 × 4 patch array utilized in [15], in this work, the scatterer array is designed for a realistic BS array with 8 × 2 and ±45° polarized antennas.
2. In addition to the single-cell simulation, an experiment in a multi-cell simulation with a typical urban micro (UMi) scenario was carefully constructed and completed to demonstrate the effectiveness of the decorrelation technique thoroughly.
3. Moreover, a real-life throughput (THP) measurement has been performed. During the measurement, the downlink (DL) THP of a 2 × 2 MIMO system is recorded (as the main performance indicator) when the user equipment (UE) moves in the testing area.

The experimental results demonstrate the effectiveness of the scatterer-array-based decorrelation method. To the authors' best knowledge, this is the first time the decorrelation method has been applied to a real BS and verified by actual THP measurements in an UMi scenario. The scatterer array shows improvement in MIMO performance without deteriorating BS's coverage. It can be integrated into the billboard or radome with a performance-boosting function, as shown in Figure 1.

MIMO performance indicators: We first briefly introduce relevant MIMO performance indicators to better understand the decorrelation method and real-life measurements.

Indictors in simulation: MIMO capacity and diversity: The MIMO capacity provides an upper bound for the data rate of an MIMO system, which can be expressed as [2]

$$C = \log_2 det\left(I + \frac{\gamma}{N} HH^H\right) \tag{1}$$

where $\boldsymbol{H}$ denotes the MIMO channel matrix, the superscript ^{H} is the Hermitian (conjugate transpose) operator, $\boldsymbol{I}$ is an identity matrix, γ is the reference signal-to-noise-ratio (SNR), and N is the number of transmitting antennas. It is usually calculated based on simulated or measured channels.

To show the correlations' effect, we resort to the well-known Kronecker channel model [2]

$$\mathbf{H} = \mathbf{R}_r^{1/2}\,\mathbf{H}_w\mathbf{R}_t^{1/2} \tag{2}$$

where $\mathbf{H}_w$ indicates the uncorrelated MIMO channel; $\mathbf{R}_r$ and $\mathbf{R}_t$ are the correlation matrices of the receiving and transmitting arrays, respectively; and the superscript $^{1/2}$ is the Hermitian square root operator with

$\mathbf{R}_r^{1/2} (\mathbf{R}_r^{1/2})^H = \mathbf{R}_r$ (taking $\mathbf{R}_r$ as an example). It is clear from Equations (1) and (2) that the correlation matrices play an essential role in the MIMO capacity, which may make the MIMO channel matrix $\mathbf{H}$ deviate from the uncorrelated spatially white MIMO channel $\mathbf{H}_w$ and thus degrade the MIMO capacity.

When there are many array elements, the correlation matrix $\mathbf{R}$ becomes large, which makes it difficult to compare the correlation performance of different MIMO arrays. Instead, it is wise to use a simple scalar, namely diversity measure (or diversity for short), to evaluate the overall correlation performance of a MIMO array, which can be calculated by [16]

$$\Psi\ (\mathbf{R}) = \left(\frac{tr\,(\mathbf{R})}{\parallel \mathbf{R} \parallel_F}\right)^2 \tag{3}$$

where $tr(\cdot)$ is the trace operator, representing the sum of the diagonal elements of a matrix, and the subscript F denotes the Frobenius norm. The diversity represents the equivalent number of uncorrelated antennas in an MIMO array. Under the premise of other factors remaining unchanged, a relatively higher diversity means a lower overall correlation of the MIMO array and, therefore, a better MIMO performance.

Indictors in real-life measurement: THP and reference signal receiving power (RSRP): The MIMO capacity shown in Equation (1) provides an upper bound for the data rate of an MIMO system based on simulated or measured channels. In comparison, the THP is the actual data rate of a practical communication system. Thus, compared with capacity, THP is a more relevant metric for the actual MIMO system, which will be used in real-life measurements.

RSRP is another essential performance indicator of a communication system, especially for testing the scatterer-array-based technique. If the scatterer array has a strong reflection, putting it in front of the BS will have a detrimental impact on the radiation patterns, lowering the receiving power in some directions. For DL THP measurements, for example, the RSRPs with and without the scatterer array remain the same, indicating that the scatterer array is well designed and maintains a good coverage. Furthermore, the THP improvement is primarily due to MIMO channel decorrelation on the BS side.

Simulation results in multipath scenarios:

BS antenna and scatterer array: The BS model used in simulations has the same aperture sizes and multiplexing as the real BS, which can mimic the performance of the real BS to some extent. Nevertheless, antenna elements' detailed structures and positions are unknown, which may cause a difference in MIMO performance between simulations and real-life measurements, as will be shown later in the following section. The BS used in the simulation is an array with 8 × 2 dual-polarized cross-dipole antennas, as shown in Figure 2. The BS antenna is modified based on the design in [17]. In particular, for miniaturization and the array's decoupling [18], a backing dielectric cavity [19] is introduced in the middle of the cross-dipoles and the metal ground. The relative permittivity of the backed dielectric cavity (i.e. the blue part in Figure 2a) is 2.65. The square FR-4 substrate (i.e. the yellow part in Figure 2a) with two cross-dipoles printed at the bottom has a thickness of 1.83 mm and a relative permittivity of 4.3. The antenna array works at 780 MHz and has an impedance bandwidth from 760 to 960 MHz with a reflection coefficient below −15 dB. The centre-to-centre distance between two nearby antennas is $0.5\lambda_0$ in the x-axis direction and 0.62 λ_0 in the y-axis direction (λ_0 denotes the wavelength in vacuum). As a typical BS setting, the antenna elements with the same polarization in the same column are excited concurrently for a higher antenna gain and a narrower beamwidth in the vertical plane (i.e. *yoz* plane).

A unit cell with a symmetrical cross pattern is designed and utilized to develop a scatterer array for the dual-polarized BS array. Each cell has two layers of metal patterns imprinted on the both side of the substrate with a relative permittivity of 6. The unit cell is optimized according to [15] to obtain a relatively higher phase shift compared to vacuum, while maintaining a good transmission coefficient magnitude when the wave is incident on the scatterer array with an angular θ in the *xoz* plane, as shown in Figure 3b. It should be noted that assuming that the other factors remain stable, the MIMO array with larger antenna element spacing tends to have relatively lower antenna correlations over a given angular spread [7]. Accordingly, the designing approach of the scatterer array tends to stretch the phase centre of antenna elements' radiation patterns away from each other, as shown in Figure 2. Therefore, it decreases the antenna correlations and increases the diversity of the MIMO array [15]. The main difference between the previous study [15] and this work is that we consider ± 45° polarized waves when designing the unit cell.

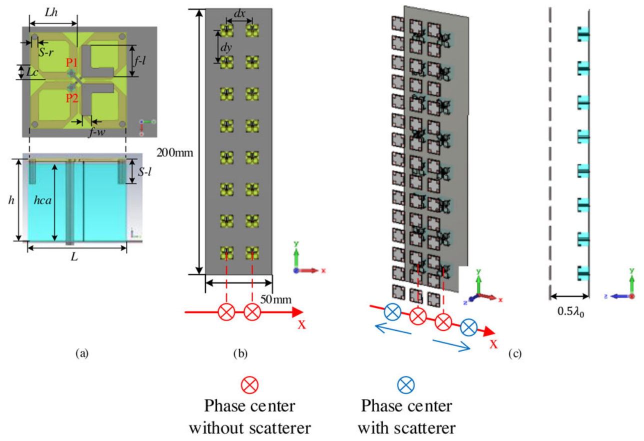

Fig. 2 *Principle of the scatterer array for decreasing antenna correlations, and (a) dual-polarized antenna with parameters:* L = 92.97, *Lc* = 14.43, *Lh* = 45.02, *S-r* = 5.73, *f-l* = 30.64, *f-w* = 8.7, *S-l* = 23.27, *h* = 77.86, *hca* = 73.28 *(unit: mm); (b) BS array with parameters: dx* = 192.3, *dy* = 238.5 *(unit: mm); (c) BS array with the scatterer array. BS, base station.*

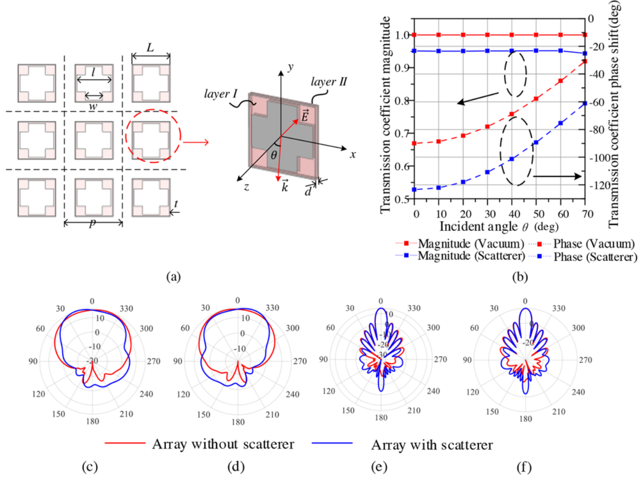

Fig. 3 *(a) Scatterer array with parameters:* L = 92.3, l = 83, w = 41.5, p = 138.5, t = 1.5, d = 6 *(unit: mm); (b) transmission magnitude and phase shift of vacuum and scatterer with the same reference surface space with a distance of $0.25\lambda_0$; embedded radiation patterns of the + 45° polarized column subarray in (c), (d)* xoz *plane and (e), (f)* yoz *plane.*

A 15 × 3 scatterer array is designed and placed in front of the BS array at a distance of about $0.5\lambda_0$, as shown in Figure 2c. For the BS array with/without the scatterer array, the embedded radiation patterns of the antenna elements are simulated in Computer Simulation Technology Studio Suite and plotted in Figures 3c to 3f. From the radiation patterns, the scatterer array has a mild effect on the horizontal plane (i.e. *xoz* plane), which means that the scatterer array does not affect the array's coverage significantly. Also, the vertical plane's (i.e. *yoz* plane) influence is negligible due to the dominance of the column phase array. Note that the increase of the equivalent phase centre distance in the presence of the scatterer array cannot be observed from the power radiation pattern. Instead, it will be reflected in the diversity enhancement in the following section.

Simulation in a single-cell scenario: To evaluate the MIMO performance in a single-cell scenario, we use a ray-tracing-based in-house

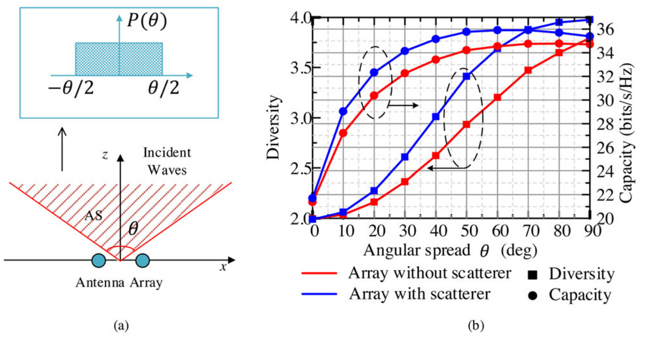

Fig. 4 *(a) Angular distribution and probability density function P(θ) of incident waves. (b) Simulated MIMO performance of the BS array with/without scatterer at 780 MHz in a single-cell scenario. BS, base station; MIMO, multiple-input multiple-output.*

Table 1. MIMO capacity enhancement due to the scatter array over 20-MHz communication bandwidth

Frequency points (MHz)	Single-cell (%)	Multi-cell (%)
770	4.04	18.75
775	4.12	19.82
780	4.22	21.29
785	4.23	22.51
790	4.7	25.39

MIMO, multiple-input multiple-output.

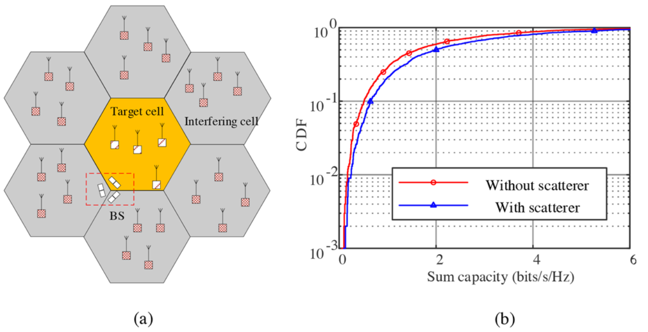

Fig. 5 *(a) Illustration of the multi-cell scenario. (b) CDF of the sum capacity of the array with/without the scatterer array in the multi-cell UMi scenario. CDF, cumulative distribution function; UMi, urban micro.*

channel emulator that has been used in [7, 15]. It is known that the angular spread (rather than the shape of the angular distribution) mainly determines the spatial correlation of an antenna de-embedded channel [20]. Thus, in simulations, we evaluate the antenna correlations (i.e. the diversity) within a varied angular spread ranging from 0° to 90° in the horizontal plane at the BS side. The channel coefficients are emulated by impinging incident waves on the embedded radiation patterns of the array elements. Moreover, the incident waves come from four uncorrelated UEs located randomly in the cell sector, and each UE has a vertically polarized dipole antenna. For one realization of the channel emulation, each UE generates 100 subpaths, and the incident waves are uniformly distributed within an angular spread at the BS side, as shown in Figure 4a. During the simulation, there are a total of 10,000 realizations for each UE and each angular spread. The diversity and channel capacity are calculated from the simulated channel coefficients and shown in Figure 4b. The capacity improvement of the BS array with the scatterer array over 20-MHz communication bandwidth at 780 MHz is shown in Table 1. As can be seen, the effectiveness of the scatterer array is clearly demonstrated in the single-cell scenario simulation.

Simulation in multi-cell scenario: Figure 5a shows an illustration of the multi-cell scenario in simulation. The scheme of the cellular layout contains seven hexagonal grids with one target cell in the middle and six

Table 2. Multi-cell simulation configuration

Parameter	Value
Number of drops	1000
Simulation scenario	UMi (NLOS)
Hexagonal cell radius	$\frac{500}{3}$ m
BS output power	40 dBm
BS height	25 m
BS array rotation	7° down tilt
UE placement	4 users per cell
UE height	1.5 m
UE speed	1 m/s

BS, base station; UE, user equipment; UMi, urban micro.

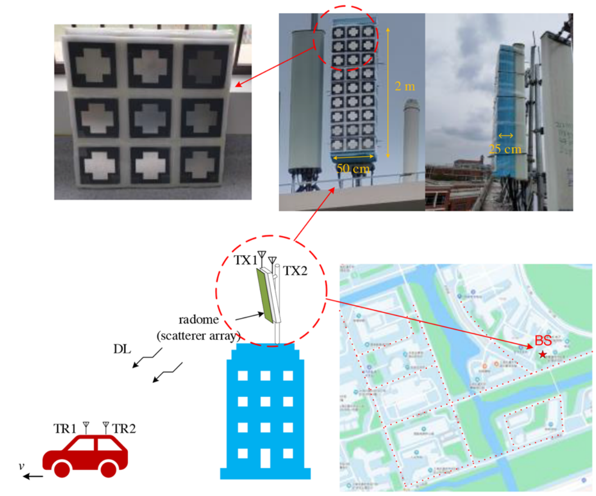

Fig. 6 *An illustration of the real-life downlink measurement with a 2 × 2 full spatial multiplexing MIMO system, photos of BS with the scatterer array, a map of the testing environment, and the UE trajectory (red dots). BS, base station; MIMO, multiple-input multiple-output.*

interfering cells surrounding the target cell. The BS is located at one vertex of the hexagon cell and has a height of 25 m above the ground with a 7° down tilt. Four UEs, each equipped with a vertically polarized dipole antenna, are randomly located in each cell sector. For link channel emulations, the geometry-based stochastic WINNER+ channel model in the UMi scenario [21] is adopted. The detailed multi-cell simulation configuration is shown in Table 2. Unlike the single-cell scenario simulation, the channel's angular spread in the multi-cell scenario is not an artificially controllable factor. Hence, the cumulative distribution function (CDF) is suitable for evaluating the performance of the MIMO array, which can show the probability of the MIMO capacity taking a value less than or equal to some specific values over whole realizations in the simulation. Figure 5b shows the CDF of the BS array with/without the scatterer array after 1000 realizations in multi-cell scenario simulation. The BS array loaded with the scatterer array has on average 21.29% improvement in the sum capacity compared with the same array without the scatterer array. The data listed in Table 1 show the capacity enhancement of the scatterer array within 20-MHz communication bandwidth. As can be seen, the scatterer array is even more effective in a multi-cell scenario as compared to the single-cell case.

Real-life measurement:

Setup of real-life measurements: Part of the scatterer array designed and fabricated for the real-life measurements according to [16] is shown in Figure 6. The scatterer array cannot be fabricated in a whole piece using the standard printed circuit broad (PCB) technology due to the huge size of the BS array to be covered. To achieve the desired periodic arrangement, each scatterer element is fabricated individually and then

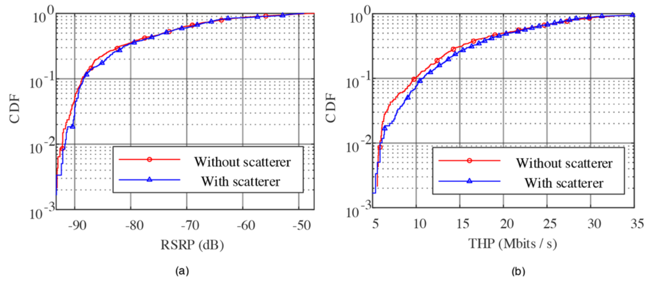

Fig. 7 *CDFs of (a) RSRP and (b) THP of the BS array with/without the scatterer array. BS, base station; CDF, cumulative distribution function; RSRP, reference signal receiving power; THP, throughput.*

embedded into a specially designed foam structure. The photos of the BS loaded with the scatterer array are shown in Figure 6. The BS array measures 2 m in height and 0.5 m in width (including the radome). It is located on the top of a building in a typical UMi scenario. Moreover, it works at 780 MHz with a communication bandwidth of 20 MHz. A 9×3 scatterer array is assembled and placed over the aperture of the BS array. The distance between the BS and the scatterer array is 25 cm. The relative permittivity of the supporting foam is close to unity. Thus, it is transparent to the BS array.

Experimental results: The CDFs of the DL RSRP and THP are plotted in Figure 7. The results show that nearly 70% of the DL THP samples show improvement by using the scatterer array, which has little impact on the power coverage of the BS.

Analyses: Comparing Figures 5b and 7b, it is found that the THP improvement in real-life measurements is not as significant as the simulated result. The reasons are given next. Firstly, the real BS has been optimized specifically for the testing environment, achieving good THP performance already. Therefore, the actual improvement brought by the scatterer array is not as significant as in the simulation. Secondly, although the real and the simulated BS arrays are similar, the detailed design information of the real BS antenna is not available. As a result, only the BS array model (cf. Figure 2) can be used to design and optimize the scatterer array. A more effective scatterer array can be designed if detailed information about the real BS antenna is available. Nevertheless, the real-life measurements show that using the scatterer array improves THP without affecting power coverage, demonstrating the effectiveness of the decorrelation technique.

Conclusion: This paper uses simulations and real-life measurements to validate the scatterer-array-based decorrelation approach. By properly designing the scatterer array, the effective inter-element spacing of the array could be enlarged and, therefore, the correlation of the adjacent antenna element in the array could be decreased, which in turn improved the MIMO performance of the BS array. The scatterer array proved effective in simulations, and the results showed obvious improvements over 20-MHz communication bandwidth in single-cell and multi-cell scenarios. Then it was applied to a real BS in a typical UMi environment for the experiment, which also showed a noticeable THP improvement without degrading the power coverage of the BS. Note that this is the first time that an effective decorrelation technique has ever been applied to a real BS, which thoroughly demonstrates the promising application potential of this technique.

Author contributions: Yipeng Wang: Methodology, Validation, Writing - original draft; Xiaoyu Huang: Validation, Investigation; Jianyao Zhao: Validation, Resources; Zhimeng Zhong: Validation, Funding acquisition; Wei E.I. Sha: Conceptualization, Resources; Xiaoming Chen: Conceptualization, Methodology, Writing - review & editing.

Acknowledgements: This work was supported by the National Key R&D Program of China under Grant 2020YFA0709800.

Conflict of interest: The authors declare no conflict of interest.

Data availability statement: Data available on request from the authors.

Received: *7 February 2023* Accepted: *11 April 2023*
doi: 10.1049/ell2.12796

References

1 Rusek, F., Persson, D., Lau, B.K., et al.: Scaling up MIMO: Opportunities and challenges with very large arrays. *IEEE Signal Process Mag.* **30**(1), 40–60 (2012)
2 Paulraj, J., Nabar, R.U., Gore, D.A.: *Introduction to Space-Time Wireless Communications*. Cambridge University Press, Cambridge (2003).
3 He, R., Ai, B., Stueber, G. L., et al.: Geometrical-based modeling for millimeter-wave MIMO mobile-to-mobile channels. *IEEE Trans. Veh. Technol.* **67**(4), 2848–2863 (2017).
4 Dey, M., Butt, M., Marchetti, N.: Throughput analysis for virtual MIMO WSNS over measured MIMO channels. *IEEE Trans. Instrum. Meas.* **68**(1), 297–299 (2019)
5 Mikki, S.M., Antar, Y.M.M.: On cross correlation in antenna arrays with applications to spatial diversity and MIMO systems. *IEEE Trans. Antennas Propag.* **63**(4), 1798–1810 (2015).
6 Qi, C., Wu, L.: Uplink channel estimation for massive MIMO systems exploring joint channel sparsity. *Electron. Lett.* **50**(23), 1770–1772 (2014)
7 Li, M., Chen, X., Zhang, A., et al.: Reducing correlation in compact arrays by adjusting near-field phase distribution for MIMO applications. *IEEE Trans. Veh. Technol.* **70**(8), 7885–7896 (2021)
8 Song, S., Da, Y., Qian, B., et al.: Dielectric resonator magnetoelectric dipole arrays with low cross polarization, backward radiation, and mutual coupling for MIMO base station applications. *China Commun.* in press.
9 Li, G., Zhai, H., Ma, Z., et al.: Isolation-improved dual-band MIMO antenna array for LTE/WIMAX mobile terminals. *IEEE Antennas Wirel. Propag. Lett.* **13**, 1128–1131 (2014)
10 Kordalivand, M., Rahman, T.A., Khalily, M.: Common elements wideband MIMO antenna system for WiFi/LTE access-point applications. *IEEE Antennas Wirel. Propag. Lett.* **13**, 1601–1604 (2014)
11 Zhu, J., Li, S., Feng, B., et al.: Compact dual-polarized UWB quasi-self-complementary MIMO/diversity antenna with band-rejection capability. *IEEE Antennas Wirel. Propag. Lett.* **15**, 905–908 (2016)
12 Quist, B.T., Jensen, M.A.: Optimal antenna radiation characteristics for diversity and MIMO systems. *IEEE Trans. Antennas Propag.* **57**(11), 3474–3481 (2009)
13 Sarkar, D., Mikki, S., Antar, Y.M.M.: Engineering the eigenspace structure of massive MIMO links through frequency-selective surfaces. *IEEE Antennas Wirel. Propag. Lett.* **18**(12), 2701–2705 (2019)
14 Caban, S., Lerch, M., Pratschner, S., et al.: Design of experiments to compare base station antenna configurations. *IEEE Trans. Instrum. Meas.* **68**(10), 3484–3493 (2019)
15 Wang, Y., Chen, X., Liu, X., et al.: Improvement of diversity and capacity of MIMO system using scatterer array. *IEEE Trans. Antennas Propag.* **70**(1), 789–794 (2022)
16 Ivrlac, M., Nossek, J., et al.: Diversity and correlation in Rayleigh fading MIMO channels. In: IEEE Vehicular Technology Conference, Stockholm, Sweden, pp. 151–155 (2005)
17 Wu, R., Chu, Q.-X.: A compact, dual-polarized multiband array for 2g/3g/4g base stations. *IEEE Trans. Antennas Propag.* **67**(4), 2298–2304 (2019)
18 Da, Y., Zhang, Z., Chen, X., et al.: Mutual coupling reduction with dielectric superstrate for base station arrays. *IEEE Antennas Wirel. Propag. Lett.* **20**(5), 843–847 (2021)
19 Li, M., Chen, X., Zhang, A., et al.: Dual-polarized broadband base station antenna backed with dielectric cavity for 5G communications. *IEEE Antennas Wirel. Propag. Lett.* **18**(10), 2051–2055 (2019)
20 Andersen, J., Pedersen, K.: Angle-of-arrival statistics for low resolution antennas. *IEEE Trans. Antennas Propag.* **50**(3), 391–395 (2002)
21 Meinilä, J., Kyösti, P., Hentilä, L., et al.: D5.3: WINNER+ final channel models (S president, 2010).